

Synthesis and Complexation of a Free Germanide Bearing a Tridentate N-Heterocyclic Substituent

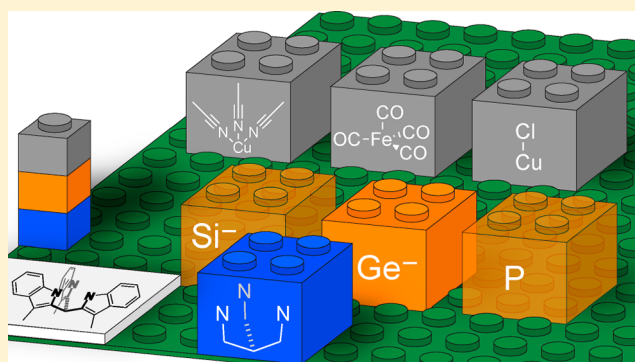
Léon Witteman,[†] Cody B. van Beek,[†] Oscar N. van Veenhuizen,[†] Martin Lutz,[‡] and Marc-Etienne Moret^{*,†}

[†]Department of Chemistry, Debye Institute for Nanomaterials Science Utrecht University, Universiteitsweg 99, 3584 CG Utrecht, The Netherlands

[‡]Crystal and Structural Chemistry, Bijvoet Center for Biomolecular Research, Faculty of Science, Utrecht University, Padualaan 8, 3584 CH Utrecht, The Netherlands

Supporting Information

ABSTRACT: The tris-N-heterocycle germanide (tmim)Ge[−] (**1**) (tmimH₃ = tris(3-methylindol-2-yl)methane) was synthesized by nucleophilic substitution for the tmim^{3−} trianion on GeCl₂·dioxane. In combination with the previously reported (tmim)Si[−] and (tmim)P analogues, it provides a convenient model for investigating the influence of the central atom on the properties of isoelectronic ligands. Complexation of the germanide (tmim)Ge[−] to CuCl resulted in the dimeric chlorocuprate [(tmim)GeCu(μ-Cl)]₂^{2−}, which is prone to dissociation in MeCN to form the neutral, solvated germylcopper (tmim)GeCu(NCMe)₃. The reaction of **1** with Fe₂(CO)₉ afforded the germyl iron tetracarbonyl [(tmim)GeFe(CO)₄][−]. Analysis of the $\tilde{\nu}(\text{CO})$ infrared absorption bands in this complex indicates that the combined electron donating and accepting properties of **1** are found in between those of (tmim)P and (tmim)Si[−]. In contrast to (tmim)Si[−], (tmim)Ge[−] is reluctant to coordinate to FeCl₂, likely because of its softer Lewis base character. Key structural features of the ligands and complexes reflect changes in their electronic properties. In particular, the N–Ge–N angles increase upon coordination to a metal fragment, suggesting increasing hybridization of the Ge s- and p-orbitals. These findings will be useful in further understanding low-valent heavier group 14 complexes in organometallic chemistry.



INTRODUCTION

Ligands based on the heavier analogues of carbenes have received considerable interest in recent years.^{1–3} A large fraction of known Si(II) and Ge(II) species are base-stabilized silylenes or germynes, i.e., compounds featuring two anionic and at least one donating, neutral substituent. Such compounds can serve as ligands for a broad range of transition metals, and transition-metal complexes of silylene^{4–11} and germylene^{5,6,10} ligands are finding applications in catalysis. Ge(II) compounds are generally less reducing than their Si(II) counterparts and hence more easily accessible, largely because Ge(II) precursors such as GeCl₂·dioxane are readily available.

Because of their similar covalent radii (Si: 1.11(2) Å and Ge: 1.20(4) Å),¹² Si(II) and Ge(II) often give rise to similar structures and parallel reactivity, but instructive differences are known. For example, Aquino et al. investigated the electronic properties, e.g., Brønsted acidity, of zwitterionic silyl-substituted methanides, silanides, and germanides (R₃E(II) anions), showing that basicity decreases down group 14 (Scheme 1, A).¹³ They also note that the methanides are markedly different from the silanides and germanides, both structurally and electronically, mainly due to significant

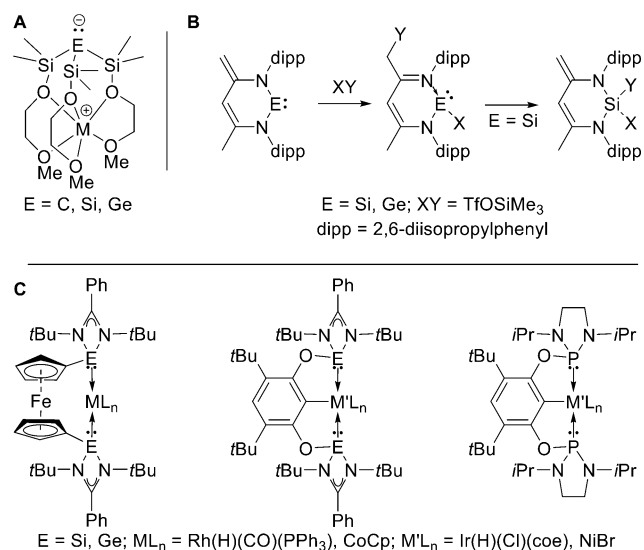
hyperconjugation of the lone pair into the adjacent silyl groups. The decreased basicity also translates in increased stability of E(II) compounds going down group 14. For example, the mere existence of compounds of type X₂E (X = halo, N(SiMe₃)₂) for E = Ge(II), Sn(II) illustrates this difference, as the Si(II) homologues decompose well below ambient temperature. The stability of these germynes and stannynes is due to the increasing energy separation of the central atom's s- and p-orbitals, descending group 14.^{14–18}

Another illustrative example is the addition of small molecules over the β -diketiminato silylene or germylene (Scheme 1, B). Despite their structural resemblance, the silylene showed a thermodynamic preference for 1,1-addition and formal oxidation of Si(II) to Si(IV), whereas, in the germylene, 1,4-addition was preferred, transforming the diamido-germylene center in a base-stabilized amido(triflate)-germylene.^{19–21} Finally, the catalytic activity of homologous silylene and germylene complexes has been compared. In hydroformylation catalysis, a rhodium complex of a ferrocene-

Received: August 30, 2018

Published: January 9, 2019

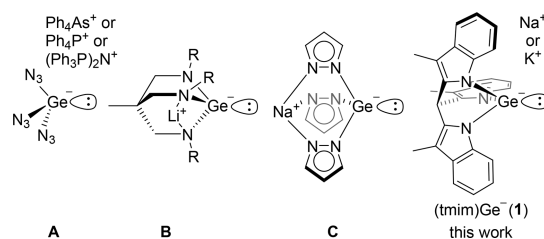
Scheme 1. (A) Group 14 Anions Used for Brønsted Acidity Determination.¹³ (B) Contrasting Reactivity between Structurally Similar Silylene and Germylene.^{19–21} (C) Catalytically Active Complexes of Silylene and Germylene Ligands and of a Related Phosphine Ligand^{5a,6,10,22}



bridged disilylene ligand (Scheme 1, C) proved to be much more active than its germylene analogue.²² This difference was attributed to the enhanced σ -donor strength of the silylene. The same trend was observed in the cyclotrimerization reaction of phenylacetylene catalyzed by the analogous CoCp complex.⁶ The decreased reactivity of the germylene complex is in this case attributed to a stronger coordination of Ge to Co, hampering the creation of an active site. Interestingly, in the C–H borylation of arenes catalyzed by an iridium SiCSi pincer complex featuring two silylene donor moieties (Scheme 1, C), the yield was only slightly higher compared to the germylene (90% and 80%), but significantly higher compared to the related phosphine complex (64%).¹⁰ The increased reactivity of the Si and Ge complexes is thought to arise from stronger σ -donor properties compared to P. Complexes of these ligands with NiBr showed similar reactivity for the silylene and phosphine in a Sonogashira coupling. Interestingly, the germylene complex showed an increased yield from 40% to 53% compared to the silylene complex.^{5a}

In recent work from our group, the synthesis and coordination chemistry of an unusual Si(II) anion supported by the tmim scaffold ($tmimH_3 = \text{tris}(3\text{-methylindol-2-yl})\text{-methane}$) by substitution on a Si(II) precursor was reported.²³ The introduction of electron-withdrawing groups to delocalize the negative charge and the tight cage structure are thought to enhance the stability of the anion by lowering the energy of the lone pair. To gain understanding on the influence of this cage design on ligand properties, the analogous germanide **1** (Chart 1) was investigated. All-nitrogen substituted germanides similar to **1** have received some attention, examples including triazidogermanide **A**, bicyclo triamidogermanide **B**, and the zwitterionic tripyrazolyl germanide **C** (Chart 1).^{24–30} Their coordination chemistry is scarce, and structurally characterized complexes are limited to a tungsten(II) complex derived from structure **A**, a gold(I) complex derived from structure **B**, and iron(II) complexes of a tetradentate triphosphinogermyl ligand.^{24–26} In the current work, the synthesis of compound **1** and its complexation to soft Lewis-acidic metal fragments

Chart 1. Naked Tri-nitrogen Substituted Germanides

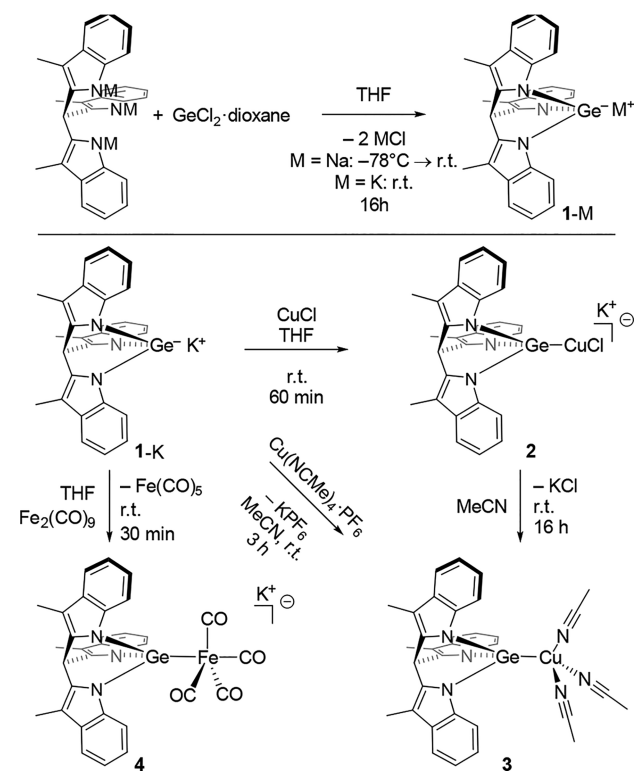


($CuCl$, $Cu(NCMe)_3$, and $Fe(CO)_4$) is reported. In contrast to the silanide, coordination to the harder Lewis acid $FeCl_2$ results in at most a weak interaction with a small association constant in solution. The properties of **1** as a ligand are compared with those of $(tmim)Si^-$ as well as the neutral P(III) analogue previously reported by Barnard and Mason,³¹ showing that its donor ability is situated between those. Analysis of the N–E–N angles, N–E, and E–M distances provides insight in the electronic nature of the ligands.

RESULTS AND DISCUSSION

The substituent $(tmim)H_3$ was synthesized and deprotonated according to published procedures.^{23,32} Subsequently, the germanide **1** was synthesized by nucleophilic substitution of chloride for the $tmim^{3-}$ trianion on $GeCl_2 \cdot \text{dioxane}$ (Scheme 2), which is a common approach to synthesize germanides.^{24–29,33,34} The germanide was obtained either as its sodium salt **1-Na** or as its potassium salt **1-K**. The synthesis of **1-Na** requires an excess of $GeCl_2 \cdot \text{dioxane}$ to reach completion, which is tentatively attributed to formation of insoluble $NaGeCl_3$. In contrast, a stoichiometric amount of $GeCl_2 \cdot$

Scheme 2. Synthesis of **1-M** by Nucleophilic Substitution of Cl for $tmim$ in $GeCl_2 \cdot \text{Dioxane}$ and Synthesis of Transition-Metal Complexes **2–4**



dioxane was sufficient for the synthesis of 1-K. Therefore, the potassium salt 1-K was used for complexation studies.

A single set of ^1H resonances in the aromatic region indicates that **1** possesses three-fold symmetry, as expected for a bicyclo[2.2.2]octane topology. The presence of **1** was detected by ESI-MS as the molecular anion (M^- (**1-K**) = measured: 474.1060 a.u., calcd: 474.1031 a.u.). Crystals of 1-Na suitable for X-ray diffraction were grown by storing a concentrated sample of 1-Na in THF at -35°C for 2 days. The molecular structure shows the presence of a free tricoordinate germanide with a solvated sodium counterion (Figure 1). The N–Ge–N angles provide a crude measure for

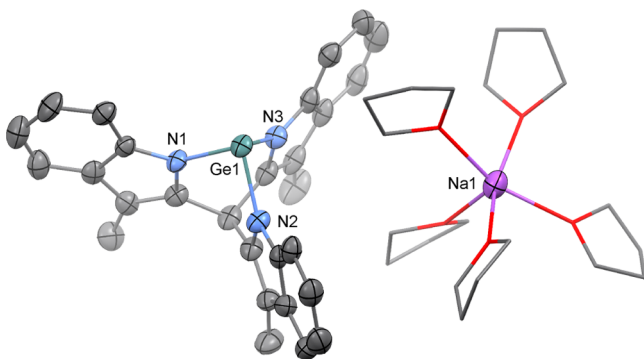


Figure 1. Molecular structure of 1-Na in the crystal. Ellipsoids are drawn at the 50% probability level. Only the major component of the disordered THF is shown. Hydrogen atoms are omitted for clarity. Selected bond distances [Å] and angles [deg]: N1–Ge1 1.956(4), N2–Ge1 1.969(4), N3–Ge1 1.970(4), N1–Ge1–N2 87.98(18), N2–Ge1–N3 88.02(18), N1–Ge1–N3 87.47(18).

the extent of hybridization of the Ge valence orbitals (s, p).³⁵ Ideally, the sum of angles is 270° in nonhybridized and 328.5° in sp^3 hybridized systems. The sum of the N–Ge–N angles ($263.5(3)^\circ$) suggests negligible hybridization of the Ge valence orbitals, with the lone pair located in the s -orbital. Angles close to 90° are commonly found in germanides, also in the absence of a cage structure enforcing them, as for example in compound **A** (Chart 1).^{27,28,36–38} This is a consequence of the generally low propensity of heavier elements to undergo orbital hybridization, i.e., the inert pair effect.^{14–18}

The coordination chemistry of the synthesized germanide was investigated with first-row transition-metal synthons (Scheme 2). Germanide 1-K was complexed to 1 equiv of CuCl in THF at ambient temperature to form the chlorocuprate **2**. A single set of ^1H resonances in the aromatic region shows retention of three-fold symmetry. In solution, the chlorocuprate exists as a monomer as was evidenced by the identical diffusion coefficients observed in DOSY NMR for **1** and **2** in $\text{C}_4\text{D}_8\text{O}$. Crystals suitable for X-ray diffraction were grown from a concentrated THF solution at -35°C . In the solid state, complex **2** has two independent dimeric Cu complexes in the asymmetric unit which are both located on general positions without symmetry. Consequently, there are four independent germanide ligands. The dimers are characterized by Cu_2Cl_2 diamond cores, similar to the (tmim)Si chlorocuprate.²³ Unlike the silicon analogue, the structure of **2** is slightly bent: the Cl–Cu–Cl planes form angles of $21.2(2)^\circ$ and $20.6(2)^\circ$ for the two independent dimers. The sum of the N–Ge–N angles in the four independent germanide ligands are $273.0(6)^\circ$, $272.7(6)^\circ$, $272.6(6)^\circ$, and $272.3(6)^\circ$. This suggests a slight

rehybridization in the direction of sp^3 compared to the free germanide **1**, for which the sum of the N–Ge–N angles is $263.5(3)^\circ$. Compound **2** constitutes only the second structurally characterized example of a germyl cuprate, next to bis(triphenylgermyl)copper as reported by Orlov et al.³⁹ Diamond core dimeric structures (Cu_2X_2 ; X = C_6F_5 , I) related to **2** were previously observed for germylene complexes bearing nacnac- and aminotroponimate ligands.^{40–42} This diamond core is generally planar; it is bent only in a Cu_2I_2 complex bearing a bidentate digermylene ligand, forcing the bent geometry.⁴³ The Ge–Cu bond lengths of 2.2557(17)–2.2611(17) Å in **2** are remarkably short, shorter distances being found only in germylene complexes of copper 1,3-diketimines.⁴⁴

The chloride in anionic cuprate **2** can be replaced by acetonitrile to form a neutral copper germanide, similarly to what is observed for the silicon analogue.²³ A saturated solution of **2** in acetonitrile produces crystals within 16 h (Figure 2). The solid-state structure of **3** shows a monomeric, tris-acetonitrile complex. This complex is one of a few neutral monodentate germyl copper complexes.^{45–48} The Ge–Cu distance in **3** (Ge1–Cu1 2.2921(3) Å) is the shortest observed for such complexes.^{45,46} To determine whether the chlorocuprate dissociates in acetonitrile and THF solution, an authentic sample of neutral **3** was synthesized by complexation of 1-K to $\text{Cu}(\text{MeCN})_4\text{PF}_6$. The ^1H NMR spectrum of the resulting complex is identical to that of **2** in CD_3CN , whereas a significant difference can be seen in the chemical shift of the indole-H7 between both samples in THF (7.62, 7.94 ppm for **3** and **2**, respectively). This suggests that complex **2** exists as a molecular chlorocuprate in THF but dissociates to the neutral complex **3** in acetonitrile.

The synthesis of an $\text{Fe}(\text{CO})_4$ derivative of compound **1** is of interest as a way to investigate its electronic properties as a ligand. Reaction of 1-K with $\text{Fe}_2(\text{CO})_9$ in THF at room temperature afforded very cleanly the $\text{Fe}(\text{CO})_4$ complex **4** (Figure 2) with loss of $\text{Fe}(\text{CO})_5$. Retention of the three-fold symmetry is indicated by a single set of ^1H NMR resonances in the aromatic region. Crystals suitable for X-ray diffraction were grown by diffusion of hexane into a concentrated THF solution of **4**. The structure is very similar to that of the neutral phosphine analogue (tmim)PFe(CO)₄ reported by Barnard and Mason.⁴⁹ The distinct axial and equatorial CO resonances of **4** in ^{13}C NMR were observed in a 1:3 ratio at -40°C (δ = 222.57, 212.16 ppm) and 1 coalesced resonance at 70°C (δ = 215.53 ppm). One broad resonance at room temperature (δ = 215.15 ppm, fwhm = 125 Hz) suggests that this is above the coalescence temperature. In (tmim)PFe(CO)₄, similar fluxional behavior was ascribed to hindered axial–equatorial exchange of the carbonyl ligands caused by steric repulsion of the indole rings on the carbonyls in the square pyramidal intermediate of plausible Berry pseudorotation⁵⁰ as well as turnstile rotation.⁴⁹ For the phosphine complex, the coalescence temperature is estimated to be 97°C , albeit not observed.³¹ The lower coalescence temperature for the germanium analogue suggests a lower energy barrier for the carbonyl exchange, which can be ascribed to the longer Ge–Fe (2.2978(16) Å) bond with respect to the P–Fe bond (2.1539(5) Å), reducing steric congestion around the iron center.

Whereas copper chloride and iron carbonyl give well-defined complexes with germanide **1**, it binds only weakly to FeCl_2 (Scheme 3). In the ^1H NMR of an equimolar solution of 1-K

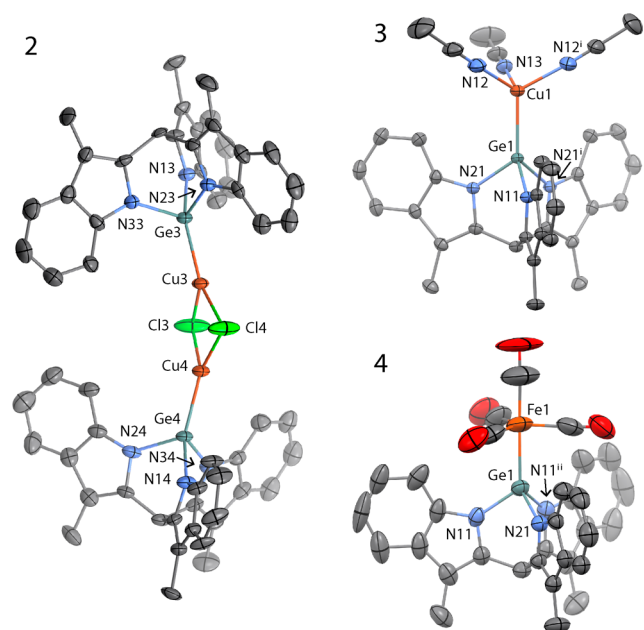
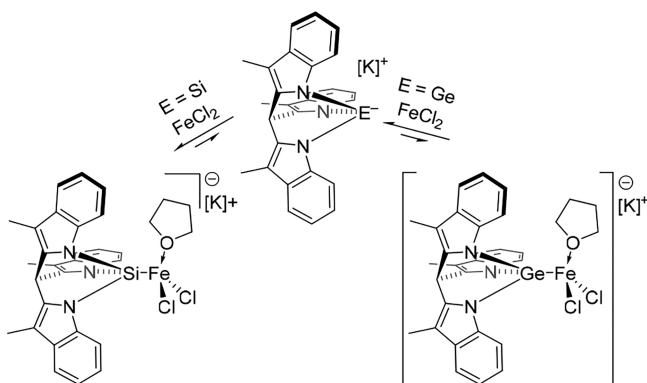


Figure 2. Molecular structure of the dianion of **2**, neutral **3**, and the anion of **4** in the crystal. Ellipsoids are drawn at the 50% probability level. Hydrogen atoms, THF solvated potassium cations, and cocrystallized, non-coordinated MeCN are omitted for clarity. Atom labels marked with ⁱ or ⁱⁱ arise from mirror symmetry. The asymmetric unit of **2** contains two independent molecules of which one is shown. Selected bond distances [Å] and angles [deg]: **2**: Molecule 1: Ge1–Cu1 2.2591(17), Ge2–Cu2 2.2557(17), Ge1–N11 1.899(8), Ge1–N21 1.898(8), Ge1–N31 1.906(9), Ge2–N12 1.911(8), Ge2–N22 1.906(9), Ge2–N32 1.918(8), N11–Ge1–N21 90.3(3), N21–Ge1–N31 91.4(4), N31–Ge1–N11 91.3(3), N12–Ge2–N22 90.6(4), N22–Ge2–N32 91.3(4), N32–Ge2–N12 90.8(3), angle between planes Cl1–Cu1–Cl2 and Cl1–Cu2–Cl2: 21.2(2). Molecule 2: Ge3–Cu3 2.2611(17), Ge4–Cu4 2.2604(16), Ge3–N13 1.907(8), Ge3–N23 1.902(9), Ge3–N33 1.901(8), Ge4–N14 1.909(8), Ge4–N24 1.917(9), Ge4–N34 1.898(9), N13–Ge3–N23 90.6(4), N23–Ge3–N33 91.4(4), N33–Ge3–N13 90.6(3), N14–Ge4–N24 90.3(3), N24–Ge4–N34 91.9(4), N34–Ge4–N14 90.1(4), angle between planes Cl3–Cu3–Cl4 and Cl3–Cu4–Cl4: 20.6(2); **3**: Ge1–Cu1 2.2921(3), Ge1–N11 1.9110(16), Ge1–N21 1.9162(11), N11–Ge1–N21 90.19(5), N21–Ge1–N21ⁱ 88.69(7) (symmetry code *i*: *x*, 1 – *y*, *z*); **4**: Ge1–Fe1 2.2978(16), Ge1–N11 1.890(5), Ge1–N21 1.902(6), N11–Ge1–N21 92.57(18), N11–Ge1–N11ⁱⁱ 92.4(3) (symmetry code *ii*: 1 – *x*, *y*, *z*).

Scheme 3. Coordination of the Silanide and Germanide Ligands to Iron Dichloride^a



^a[K]⁺ = K(18-crown-6)⁺ for E = Si and K⁺ for E = Ge.

and FeCl₂ in THF, the indole-H7 peak broadens (fwhm, from 2.8 to 40 Hz) and shifts 0.50 ppm to low field (Figure 3).

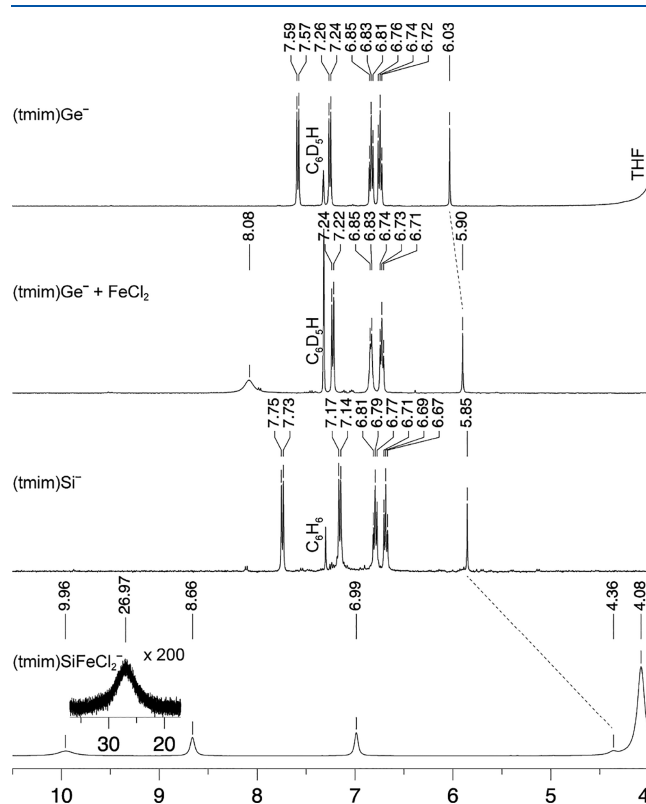


Figure 3. ¹H NMR spectra of (tmim)E[−] compounds (E = Ge, Si, SiFeCl₂) and an equimolar mixture of **1**-K and FeCl₂ in THF-H₈ + C₆D₆ (Ge) or THF-d₈ (Si).

Concomitantly, the R₃CH signal shifts 0.13 ppm to high field. This is in contrast with (tmim)Si[−], which binds to FeCl₂ to form (tmim)SiFeCl₂·THF, causing a low-field shift of 20 ppm for the indole-H7 and a high-field shift of 1.5 ppm for the R₃CH signal.²³ The weaker affinity of **1** for FeCl₂ with respect to (tmim)Si[−] can be understood in terms of Hard and Soft Acids and Bases (HSAB), the germanide being a softer Lewis base than the silanide.

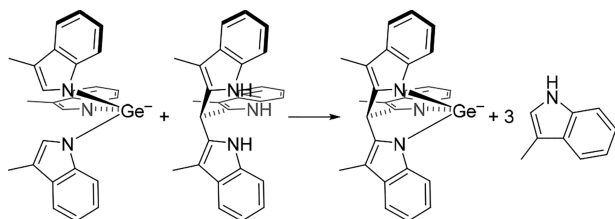
The series of Ge compounds described herein provide a rare opportunity to compare side by side the properties of isostructural ligands featuring three different central elements, namely, P(III),^{31,49} Si(II),²³ and Ge(II). Key geometrical and spectroscopic parameters are collected in Table 1. In the solid state, the anions (tmim)Ge[−] and (tmim)Si[−] possess rather acute N–E–N angles (Σ(N–Si–N) = 272.58(9)°, Σ(N–Ge–N) = 263.5(3)°, with respect to the phosphine analogue (Σ(N–P–N) = 285.30(12)°, Table 1).^{31,49} The more acute angles in (tmim)Ge[−] compared to (tmim)Si[−] likely arise from the larger atomic radius of germanium, because the through-space N⋯CH⋯N angles are larger in (tmim)Ge[−], indicating that the tmim scaffold needs to open up to accommodate the larger Ge[−] anion. This is also reflected in the N–E distances being larger in (tmim)Ge[−], but does not appear to result in substantial cage strain. The strain energy estimated computationally for (tmim)Ge[−] according to the homodesmotic reaction depicted in Scheme 4 is very low (ΔH = −1.0 kcal/mol), similarly to those calculated for (tmim)Si[−] (−1.6 kcal/mol) and (tmim)P (1.2 kcal/mol; Supporting Information, Table S2).²³ The difference in N–E–N angles between Si and

Table 1. Sum of Angles, Distances, and $\tilde{\nu}(\text{CO})$ in tmimE Compounds (E = P, Si[−], Ge[−]) and Their Complexes

E =	P	Si [−]	Ge [−]
tmimE			
ΣN–E–N/deg	285.30(12)	272.58(9)	263.5(3)
⟨N–E⟩/Å	1.7084(8)	1.8416(6)	1.965(2)
⟨N...CH...N⟩/deg	62.3	64.7	67.40(12)
[(tmimE)Cu(μ-Cl)] ₂ ^{2−}			
Cu–E/Å		2.1906(10)	2.2557(17)–2.2611(17) ^b
ΣN–E–N/deg		280.8(2)	272.3(3)–273.0(6) ^b
⟨N–E⟩/Å		1.8010(17)	1.901(5)–1.912(5) ^b
(tmimE)Cu(NCMe) ₃			
Cu–E/Å		2.2106(8)	2.2921(3)
ΣN–E–N/deg		278.73(12)	269.07(12)
⟨N–E⟩/Å		1.8063(10)	1.9145(7)
(tmimE)Fe(CO) ₄			
Fe–E/Å	2.1539(5)		2.2978(16)
ΣN–E–N/deg	292.56(12)		277.5(4)
⟨N–E⟩/Å	1.7085(8)		1.894(3)
$\tilde{\nu}(\text{CO})/\text{cm}^{-1}$ exp	2076 2006 1977	2029 ^a 1920	2037 1954 1933
$\tilde{\nu}(\text{CO})/\text{cm}^{-1}$ calcd	2074 2012 1990	2026 1956 1939	2032 1961 1948

^aTentative assignment from a spectrum measured on a mixture of components. ^bFour independent germanide ligands.

Scheme 4. Homodesmotic Reaction Used for Strain Calculations²³



P is likely a combined effect of the slightly larger P radius and the absence of a negative charge on phosphorus, i.e., less repulsion for the anionic indole moieties.

The solid-state structures of the complexes presented herein correlate with changes in orbital hybridization at the central atom. Upon complexation, the N–E–N angles increase in all ligands, which can be explained by an increasing p-character of the lone pair upon binding to a Lewis acid and a consequent decrease in the p-character of the E–N bonding orbitals. This is in agreement with Bent's rule: increased electronegativity of a substituent (from a lone pair to a metal fragment) results in increased p-character of the bonding orbitals.³⁵ The E–N distances decrease upon complexation for both (tmim)Si and **1** to CuCl and Cu(MeCN)₃, but the E–N distances in (tmim)P remain unchanged within the error bounds upon complexation to Fe(CO)₄. This difference can be interpreted as a consequence of the stronger electron-donor character of the anionic ligands as compared with (tmim)P, which results in a higher degree of charge transfer upon complexation, causing a shortening of the N–E bonds as the electron density at the central element is depleted.

In the cuprates derived from (tmim)Ge[−] and (tmim)Si[−], the E–Cu distances are very short and congruent ($\Delta d(\text{E}–\text{Cu}) = 0.0686(13)$ Å) if one takes into account the difference in covalent radii between Si and Ge (0.09(4) Å).¹² The metal fragment in the acetonitrile complexes is somewhat less electron-withdrawing as is reflected in tightening of the N–E–N angles and a slight increase in E–N distance from LCuCl[−] to LCu(NCMe)₃, correlating with slightly longer Cu–

E bonds. This can be taken to indicate that the increase in coordination number in the acetonitrile complex outweighs the loss of the more electron-rich, anionic chloride ligand.

For comparison with **4**, complexation of (tmim)Si[−] to Fe(CO)₄ was investigated. It affords a mixture of two major components of which one is tentatively assigned to [(tmim)SiFe(CO)₄][−] on the basis of ESI-MS and IR (in combination with DFT-calculated $\tilde{\nu}(\text{CO})$, Table 1). Isolation of the silyl iron complex was unsuccessful. The vibrational frequency of the carbonyls in (tmim)EFe(CO)₄ (E = Si[−], Ge[−], P; Table 1) indicates that the silanide is the strongest electron donor, the germanide is somewhat weaker, and the phosphine is a significantly weaker donor.

CONCLUSIONS

The free germanide (tmim)Ge[−] (**1**, (tmim)H₃ = tris(3-methylindol-2-yl)methane) was synthesized through nucleophilic substitution on GeCl₂·dioxane by the trianion tmim^{3−}. Germanide **1** was shown to coordinate to Cu(I) and Fe(0) fragments, affording the chloro cuprate [(tmim)GeCuCl][−] and the iron carbonyl complex [(tmim)GeFe(CO)₄][−]. The chloro cuprate was shown to dissociate in acetonitrile to give the neutral acetonitrile solvated complex (tmim)GeCu(NCMe)₃. Contrasting with the reactivity of the analogous silanide, coordination of **1** to FeCl₂ results in at most a weak interaction. With the existence of the analogous (tmim)P and (tmim)Si[−], and complexes thereof, a rare opportunity arose of comparing the properties of isostructural ligands featuring different central elements, namely, P(III), Si(II), and Ge(II). The relative electron donor strength was interrogated from the observed $\tilde{\nu}(\text{CO})$ in IR spectroscopy, showing that the donor strength follows the trend $P < \text{Ge} < \text{Si}$. Analysis of the N–E–N angles, N–E, and E–M distances provides insight in the electronic nature of the ligands, suggesting increased hybridization of the Ge s- and p-orbitals upon complexation to a metal fragment. The findings presented here contribute to the understanding of low-valent heavier group 14 ligands and their complexes and may provide important insights necessary for further development of this promising class of ligands.

EXPERIMENTAL SECTION

All reactions involving air-sensitive compounds were conducted under a N₂ atmosphere by using standard glovebox or Schlenk techniques. Acetonitrile and *n*-hexane were dried with an MBRAUN MB SPS-79 system; THF was distilled from benzophenone/Na. All solvents were degassed by bubbling with N₂ for 30 min, and stored over molecular sieves in a glovebox. Deuterated acetonitrile and THF were degassed by four freeze–pump–thaw cycles and stored over molecular sieves in a glovebox. Skatole, NaH (60 wt % in mineral oil), KH (30 wt % in mineral oil), and FeCl₂ were purchased from Sigma-Aldrich. Triethyl orthoformate, Fe₂(CO)₉, and CuCl were purchased from Acros. GeCl₂·dioxane was purchased from ABCR. All commercially obtained chemicals were used as received, except for CuCl. From CuCl, copper oxides and hydroxides were removed with hydrochloric acid as described in the literature, and the resulting solid was azeotropically dried with acetonitrile until $\tilde{\nu}(\text{C}\equiv\text{N})$ in the IR spectrum disappeared.⁵¹ All NMR measurements were performed on a Varian VNMR400 or Varian MRF400 spectrometer; shifts are reported relative to TMS with the residual solvent signal as internal standard.⁵² All NMR experiments involving air-sensitive compounds were conducted in J-Young NMR tubes under a N₂ atmosphere. Salts of solvated sodium or potassium cations generally yielded unreliable elemental analysis data due to partial desolvation. Their purity was established by NMR spectroscopy. In particular, the THF content determination for purity purposes was done by NMR; the acquisition time was chosen so that the full FID was recorded. Additionally, the relaxation time was set to 7 times the longest T₁, determined by an individual T₁ measurement. IR spectra were recorded on a PerkinElmer Spectrum Two FT-IR spectrometer. ESI-MS measurements were performed on a Waters LCT Premier XE KE317 spectrometer; the Waters software was used for simulations. Elemental analysis was conducted by the Mikroanalytisches Laboratorium Kolbe (3, 4) or Medac Ltd. (2). The experimental methods and parameters of the X-ray crystal structure determinations are detailed in the Supporting Information. The compounds (tmim)H₃,³² (tmim)Na₃,²³ (tmim)K₃,²³ and (tmim)Si^{−23} were prepared according to reported procedures.

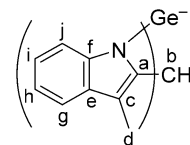
Computational Methods. Calculations were performed using Gaussian 09, Revision D.01.⁵³ The absence of negative eigenvalues was confirmed for all structures. All structures were optimized using the TPSS functional with the TZVP basis set.

Syntheses. *Synthesis of Na[(tmim)Ge] (1-Na).* Solutions of (tmim)Na₃ (501 mg, 27 wt % THF, 0.78 mmol) in THF (10 mL) and GeCl₂·dioxane (337 mg, 1.46 mmol) in THF (6 mL) were cooled to −78 °C. The GeCl₂·dioxane solution was added to the stirred tmim solution, resulting in a suspension. This was allowed to warm to r.t. over 16 h. Filtration and removal of the solvent, followed by recrystallization from THF at −35 °C and drying *in vacuo*, afforded a yellow powder (190 mg, 34 wt % THF, 0.405 mmol, 32%). ¹H NMR (400 MHz, CD₃CN, 25 °C) δ = 7.56 (dt, ³J(H,H) = 8.3 Hz, ⁴J(H,H) = 0.8 Hz, ⁵J(H,H) = 0.8 Hz, 3H, Indole-H7), 7.32 (dt, ³J(H,H) = 7.8 Hz, ⁴J(H,H) = 1.1 Hz, ⁵J(H,H) = 1.1 Hz, 3H, Indole-H4), 6.92 (ddd, ³J(H,H) = 8.1 Hz, ³J(H,H) = 7.0 Hz, ⁴J(H,H) = 1.3 Hz, 3H, Indole-H6), 6.83 (ddd, ³J(H,H) = 7.9 Hz, ³J(H,H) = 7.0 Hz, ⁴J(H,H) = 1.1 Hz, 3H, Indole-H5), 6.01 (s, 1H, R₃CH), 2.43 ppm (s, 9H, CH₃). ¹³C NMR (101 MHz, CD₃CN, 25 °C) δ = 141.9 (2x ^{Ar}qC), 131.2 (^{Ar}qC), 119.9 (^{Ar}CH), 118.6 (^{Ar}CH), 117.7 (^{Ar}CH), 112.2 (^{Ar}CH), 103.4 (^{Ar}qC), 34.2 (R₃CH), 8.9 ppm (CH₃). Satisfactory elemental analysis could not be obtained, likely due to THF solvation.

Synthesis of (tmim)GeK (1-K). A solution of GeCl₂·dioxane (203 mg, 0.875 mmol) in THF (6 mL) was added over 20 min at room temperature to an orange, green luminescent solution of (tmim)K₃ (500 mg, 10 wt % THF, 0.869 mmol) in THF (15 mL) and stirred for 16 h. The resulting yellow suspension was diluted to 40 mL with THF and centrifuged for 10 min at 2000 rpm. The decanted supernatant was concentrated to 6 mL, during which precipitation occurred. Decanting and washing with THF (4 × 0.5 mL) yielded a white microcrystalline powder (297 mg). Repeated storing of the combined THF fractions at −35 °C for 16 h, decanting, and washing with cold

THF yielded two more crops (m_{total} = 506 mg, 37 wt % THF, 0.62 mmol, 71%). ¹H NMR (400 MHz, CD₃CN, 25 °C) δ = 7.58 (dt, ³J(H,H) = 8.1 Hz, ⁴J(H,H) = 0.9 Hz, ⁵J(H,H) = 0.9 Hz, 3H, Indole-H7), 7.34 (dt, ³J(H,H) = 7.8 Hz, ⁴J(H,H) = 1.0 Hz, ⁵J(H,H) = 1.0 Hz, 3H, Indole-H4), 6.94 (ddd, ³J(H,H) = 8.1 Hz, ³J(H,H) = 6.9 Hz, ⁴J(H,H) = 1.3 Hz, 3H, Indole-H6), 6.85 (ddd, ³J(H,H) = 7.9 Hz, ³J(H,H) = 7.0 Hz, ⁴J(H,H) = 1.1 Hz, 3H, Indole-H5), 6.03 (s, 1H, R₃CH), 2.46 ppm (s, 9H, CH₃). ¹H NMR (400 MHz, C₄D₈O + C₆D₆, 25 °C) δ = 7.54 (d, ³J(H,H) = 8.0 Hz, 3H, Indole-H7), 7.21 (d, ³J(H,H) = 7.7 Hz, 3H, Indole-H4), 6.79 (t, ³J(H,H) = 7.5 Hz, 3H, Indole-H6), 6.70 (t, ³J(H,H) = 7.3 Hz, 3H, Indole-H5), 5.99 (s, 1H, R₃CH), 2.41 ppm (s, 9H, CH₃). ¹³C NMR (Chart 2 gives a graphical

Chart 2. Assignment of ¹³C NMR Signals of (tmim)Ge[−] (1)



depiction of the assignment) (101 MHz, CD₃CN, 25 °C) δ = 142.0 (C_d), 141.9 (C_e), 131.2 (C_f), 120.0 (C_g), 118.6 (C_h), 117.7 (C_i), 112.2 (C_j), 103.4 (C_k), 34.2 (C_l), 8.9 ppm (C_m). DOSY NMR (400 MHz, C₄D₈O, 25 °C): D = 7 × 10^{−18} m²/s; ESI-MS C₂₈H₂₂N₃Ge[−]: exp: 474.1060, sim: 474.1031 a.u. Satisfactory elemental analysis could not be obtained, likely due to THF solvation.

Synthesis of K[(tmim)GeCu] (2). To the combined solids 1-K (30 mg, 40 wt % THF, 35 μmol) and CuCl (3.5 mg, 35 μmol) was added THF (2 mL), and the suspension was stirred for 60 min, during which the amount of solid increased. The resulting suspension was freed of solvent *in vacuo*, affording a white powder (29 mg, 27 wt % THF, 35 μmol, 99%). ¹H NMR (400 MHz, C₄D₈O, 25 °C) δ = 7.96 (d, ³J(H,H) = 8.1 Hz, 3H, Indole-H7), 7.26 (d, ³J(H,H) = 7.7 Hz, 3H, Indole-H4), 6.90 (t, ³J(H,H) = 7.5 Hz, 3H, Indole-H6), 6.77 (t, ³J(H,H) = 7.4 Hz, 3H, Indole-H5), 6.05 (s, 1H, R₃CH), 2.43 ppm (s, 9H, CH₃). ¹³C NMR (101 MHz, C₄D₈O, 25 °C) δ = 140.5 (^{Ar}qC), 139.8 (^{Ar}qC), 130.6 (^{Ar}qC), 118.9 (^{Ar}CH), 117.3 (^{Ar}CH), 116.8 (^{Ar}CH), 111.5 (^{Ar}CH), 102.8 (^{Ar}qC), 32.7 (R₃CH), 7.8 ppm (CH₃). DOSY NMR (400 MHz, C₄D₈O, 25 °C): D = 7 × 10^{−18} m²/s; ESI-MS C₂₈H₂₂N₃ClGeCu[−]: exp: 572.0092, sim: 572.0009 a.u. Satisfactory elemental analysis could not be obtained, likely due to THF solvation.

Solvolysis of 2 To Form (tmim)GeCu(MeCN)₃ (3). A solution of 2 (~10 mg) in CD₃CN (0.4 mL) was allowed to stand for 16 h, during which crystals of 3 suitable for X-ray diffraction grew. ¹H NMR (400 MHz, CD₃CN, 25 °C) δ = 7.78 (d, ³J(H,H) = 8.1 Hz, 3H, Indole-H7), 7.34 (ddd, ³J(H,H) = 7.7 Hz, ⁴J(H,H) = 1.3 Hz, ⁵J(H,H) = 0.7 Hz, 3H, Indole-H4), 6.94 (t, ³J(H,H) = 7.5 Hz, 3H, Indole-H6), 6.87 (ddd, ³J(H,H) = 7.9 Hz, ³J(H,H) = 6.9 Hz, ⁴J(H,H) = 1.1 Hz, 3H, Indole-H5), 6.04 (s, 1H, R₃CH), 2.42 ppm (s, 9H, CH₃). ¹³C NMR (101 MHz, CD₃CN, 25 °C) δ = 141.4 (^{Ar}qC), 140.8 (^{Ar}qC), 131.1 (^{Ar}qC), 120.7 (^{Ar}CH), 118.9 (^{Ar}CH), 118.5 (^{Ar}CH), 112.5 (^{Ar}CH), 104.7 (^{Ar}qC), 33.6 (R₃CH), 8.7 ppm (CH₃).

Synthesis of (tmim)GeCu(MeCN)₃ (3) from Cu(MeCN)₄PF₆. A solution of 1-K (32 mg, 38 wt % THF, 39 μmol) in acetonitrile (0.5 mL) was added to a stirred solution of Cu(MeCN)₄PF₆ (14 mg, 39 μmol) in acetonitrile (0.5 mL). The vial was rinsed with acetonitrile (2 × 0.5 mL), and the solution was added to the mixture. Within 5 min, a white solid precipitated. After 3 h, the mixture was filtered and the white residue was washed with acetonitrile (2 × 0.5 mL) and freed of solvent *in vacuo* (21 mg, 32 μmol, 83%). ¹H NMR (400 MHz, C₄H₈O + C₆D₆, 25 °C) δ = 7.62 (d, ³J(H,H) = 8.0 Hz, 3H, Indole-H7), 7.28 (d*, Indole-H4), 6.86 (t, ³J(H,H) = 7.5 Hz, 3H, Indole-H6), 6.79 (t, ³J(H,H) = 7.3 Hz, 3H, Indole-H5), 6.04 (s, 1H, R₃CH), 2.42 ppm (s, 9H, CH₃). *doublet overlaps with C₆D₆H. ¹H NMR (400 MHz, CD₃CN, 25 °C) δ = 7.77 (d, ³J(H,H) = 8.1 Hz, 3H, Indole-H7), 7.34 (d, ³J(H,H) = 7.7 Hz, 3H, Indole-H4), 6.94 (t, ³J(H,H) = 7.5 Hz, 3H, Indole-H6), 6.87 (t, ³J(H,H) = 7.3 Hz, 3H,

Indole-**H5**), 6.04 (s, 1H, R₃CH), 2.42 ppm (s, 9H, CH₃). ¹³C NMR (101 MHz, CD₃CN, 25 °C) δ = 141.4 (ArqC), 140.8 (ArqC), 131.1 (ArqC), 120.7 (ArCH), 118.9 (ArCH), 118.5 (ArCH), 112.4 (ArCH), 104.7 (ArqC), 33.6 (R₃CH), 8.7 ppm (CH₃). Satisfactory elemental analysis could not be obtained, likely due to loss of coordinated MeCN.

Synthesis of K[(tmim)GeFe(CO)₄] (4). A solution of 1-K (122 mg, 62 wt % THF, 0.15 mmol) in THF (13 mL) was added to an orange suspension of Fe₂(CO)₉ (54 mg, 147 μmol) in THF (5 mL) and stirred for 30 min. The solution was freed of solvent *in vacuo* to a burgundy solid, which was dissolved in THF (1.5 mL) and cooled to −35 °C. Cold hexane (15 mL) was added, and after 16 h at −35 °C, the suspension was filtered and the white solid was dried *in vacuo* (105 mg, 15 wt % THF, 0.13 mmol, 88%). ¹H NMR (400 MHz, CD₃CN, 70 °C) δ = 8.00 (d, ³J(H,H) = 8.2 Hz, 3H), 7.41 (d, ³J(H,H) = 7.8 Hz, 3H), 7.04 (ddd, ³J(H,H) = 8.3 Hz, ³J(H,H) = 6.8 Hz, ⁴J(H,H) = 1.5 Hz, 3H), 6.96 (t, ³J(H,H) = 7.4 Hz, 3H), 6.17 (s, 1H), 2.49 ppm (s, 8H). ¹H NMR (400 MHz, CD₃CN, 25 °C) δ = 7.96 (dt, ³J(H,H) = 8.3 Hz, ⁴J(H,H) = 0.9 Hz, 3H, Indole-**H7**), 7.40 (ddd, ³J(H,H) = 7.8 Hz, ⁴J(H,H) = 1.3 Hz, ⁵J(H,H) = 0.7 Hz, 3H, Indole-**H4**), 7.04 (ddd, ³J(H,H) = 8.3 Hz, ³J(H,H) = 7.0 Hz, ⁴J(H,H) = 1.3 Hz, 3H, Indole-**H6**), 6.95 (ddd, ³J(H,H) = 7.9 Hz, ³J(H,H) = 7.0 Hz, ⁴J(H,H) = 1.1 Hz, 3H, Indole-**H5**), 6.15 (s, 1H), 2.46 ppm (s, 9H). ¹H NMR (400 MHz, CD₃CN, −40 °C) δ = 7.94 (dt, ³J(H,H) = 8.3 Hz, ⁴J(H,H) = 0.9 Hz, 3H), 7.40 (ddd, ³J(H,H) = 7.8 Hz, ⁴J(H,H) = 1.3 Hz, ⁵J(H,H) = 0.7 Hz, 3H), 7.04 (ddd, ³J(H,H) = 8.3 Hz, ³J(H,H) = 7.0 Hz, ⁴J(H,H) = 1.3 Hz, 3H), 6.95 (ddd, ³J(H,H) = 7.9 Hz, ³J(H,H) = 7.0 Hz, ⁴J(H,H) = 1.1 Hz, 3H), 6.15 (s, 1H), 2.45 ppm (s, 9H). ¹³C NMR (101 MHz, CD₃CN, −40 °C): δ = 222.6 (ArCO), 212.2 (ArCO), 140.3 (ArqC), 139.0 (ArqC), 130.4 (ArqC), 121.3 (ArCH), 119.0 (2 ArCH), 112.2 (ArCH), 105.6 (ArqC), 32.4 (R₃CH), 8.4 ppm (CH₃). ¹³C NMR (101 MHz, CD₃CN, 25 °C): δ = 215.1 (fwhm = 125 Hz, CO), 141.0 (ArqC), 139.9 (ArqC), 131.2 (ArqC), 121.5 (ArCH), 119.3 (ArCH), 119.2 (ArCH), 112.9 (ArCH), 105.6 (ArqC), 33.1 (R₃CH), 8.6 ppm (CH₃). ¹³C NMR (101 MHz, CD₃CN, 70 °C): δ = 215.5 (CO), 141.6 (ArqC), 140.5 (ArqC), 131.8 (ArqC), 121.6 (ArCH), 119.5 (ArCH), 119.4 (ArCH), 113.3 (ArCH), 105.7 (ArqC), 33.7 (R₃CH), 8.8 ppm (CH₃); ESI-MS C₃₂H₂₂O₄GeN₃Fe[−]: exp: 642.0437, sim: 642.0180 a.u.; IR (THF): $\tilde{\nu}$ = 2037, 1954, 1933 cm^{−1}. Satisfactory elemental analysis could not be obtained, likely due to THF solvation.

Interaction between 1 and FeCl₂. The combined solids 1-K (30 mg, 40 wt % THF, 35 μmol) and FeCl₂ (4.6 mg, 36 μmol) were dissolved in THF (2 mL) and stirred for 60 min. ¹H NMR (400 MHz, C₆D₆O + C₆D₆, 25 °C) δ* = 8.08 (br s, 3H), 7.23 (d, ³J(H,H) = 7.6 Hz, 3H), 6.83 (br d, ³J(H,H) = 6.8 Hz, 3H), 6.73 (t, ³J(H,H) = 7.1 Hz, 3H), 5.90 (s, 1H), 2.40 ppm (s, 9H). * relative to C₆D₅H in THF (7.32 ppm).

■ ASSOCIATED CONTENT

■ Supporting Information

The Supporting Information is available free of charge on the ACS Publications website at DOI: 10.1021/acs.organomet.8b00630.

Crystallographic data, spectroscopic data, and computational details (PDF)

Coordinates of the computed structures (XYZ)

Accession Codes

CCDC 1848178–1848181 contain the supplementary crystallographic data for this paper. These data can be obtained free of charge via www.ccdc.cam.ac.uk/data_request/cif, or by emailing data_request@ccdc.cam.ac.uk, or by contacting The Cambridge Crystallographic Data Centre, 12 Union Road, Cambridge CB2 1EZ, UK; fax: +44 1223 336033.

■ AUTHOR INFORMATION

Corresponding Author

*E-mail: M.Moret@uu.nl.

ORCID

Léon Witteman: 0000-0003-2189-830X

Marc-Etienne Moret: 0000-0002-3137-6073

Notes

The authors declare no competing financial interest.

■ ACKNOWLEDGMENTS

Support with NMR spectroscopic analysis by Dr. J. T. B. H. Jastrzebski is gratefully acknowledged. We acknowledge funding from the European Union Seventh Framework Programme (FP7/2007–2013) under grant agreement PIIF-GA-2012-327306 (IIF-Marie Curie grant awarded to M.-E.M.), the Dutch National Research School Combination Catalysis (NRSC-C), and the Sectorplan Natuur- en Scheikunde (Tenure-track grant at Utrecht University). This work was sponsored by NWO Exacte en Natuurwetenschappen (Physical Sciences) for the use of supercomputer facilities, with financial support from The Netherlands Organization for Scientific Research (NWO). The X-ray diffractometer was financed by the NWO.

■ REFERENCES

- (1) Benedek, Z.; Szilvási, T. Theoretical Assessment of Low-Valent Germanium Compounds as Transition Metal Ligands: Can They Be Better than Phosphines or NHCs? *Organometallics* **2017**, *36*, 1591–1600.
- (2) Benedek, Z.; Szilvási, T. Can Low-Valent Silicon Compounds Be Better Transition Metal Ligands than Phosphines and NHCs? *RSC Adv.* **2015**, *5*, 5077–5086.
- (3) Kilian, M.; Wadepohl, H.; Gade, L. H. Triamidostannates(II) as Sterically Demanding Ligands for Rhodium and Iridium. *Organometallics* **2008**, *27*, 524–533.
- (4) Fürstner, A.; Krause, H.; Lehmann, C. W. Preparation, Structure and Catalytic Properties of a Binuclear Pd(0) Complex with Bridging Silylene Ligands. *Chem. Commun.* **2001**, *80*, 2372–2373.
- (5) (a) Gallego, D.; Brück, A.; Irran, E.; Meier, F.; Kaupp, M.; Driess, M.; Hartwig, J. F. From Bis(Silylene) and Bis(Germylene) Pincer-Type Nickel(II) Complexes to Isolable Intermediates of the Nickel-Catalyzed Sonogashira Cross-Coupling Reaction. *J. Am. Chem. Soc.* **2013**, *135*, 15617–15626. (b) Álvarez-Rodríguez, L.; Cabeza, J. A.; García-Álvarez, P.; Pérez-Carreño, E. Ruthenium Carbene Complexes Analogous to Grubbs-I Catalysts Featuring Germylenes as Ancillary Ligands. *Organometallics* **2018**, *37*, 3399–3406. (c) Álvarez-Rodríguez, L.; Cabeza, J. A.; Fernández-Colinas, J. M.; García-Álvarez, P.; Polo, D. Amidinatogermylene Metal Complexes as Homogeneous Catalysts in Alcoholic Media. *Organometallics* **2016**, *35*, 2516–2523. (d) Sharma, M. K.; Singh, D.; Mahawar, P.; Yadav, R.; Nagendran, S. Catalytic cyanosilylation using germylene stabilized platinum(II) dicyanide. *Dalton Trans.* **2018**, *47*, 5943–5947.
- (6) Wang, W.; Inoue, S.; Enthaler, S.; Driess, M. Bis(Silylenyl) and Bis(Germynyl) Substituted Ferrocenes: Synthesis, Structure, and Catalytic Applications of Bidentate Silicon(II)–Cobalt Complexes. *Angew. Chem., Int. Ed.* **2012**, *51*, 6167–6171.
- (7) Metsänen, T. T.; Gallego, D.; Szilvási, T.; Driess, M.; Oestreich, M. Peripheral Mechanism of a Carbonyl Hydrosilylation Catalysed by an SiNSi Iron Pincer Complex. *Chem. Sci.* **2015**, *6*, 7143–7149.
- (8) Gallego, D.; Inoue, S.; Blom, B.; Driess, M. Highly Electron-Rich Pincer-Type Iron Complexes Bearing Innocent Bis(Metallylene)-Pyridine Ligands: Syntheses, Structures, and Catalytic Activity. *Organometallics* **2014**, *33*, 6885–6897.
- (9) Zhang, M.; Liu, X.; Shi, C.; Ren, C.; Ding, Y.; Roesky, H. W. The Synthesis of (η³-C₃H₅)Pd{Si[N(tBu)CH₃]₂}Cl and the Catalytic

Property for Heck Reaction. *Z. Anorg. Allg. Chem.* **2008**, 634, 1755–1758.

(10) Brück, A.; Gallego, D.; Wang, W.; Irran, E.; Driess, M.; Hartwig, J. F. Pushing the σ -Donor Strength in Iridium Pincer Complexes: Bis(Silylene) and Bis(Germylene) Ligands Are Stronger Donors than Bis(Phosphorus(III)) Ligands. *Angew. Chem., Int. Ed.* **2012**, 51, 11478–11482.

(11) Blom, B.; Enthaler, S.; Inoue, S.; Irran, E.; Driess, M. Electron-Rich N-Heterocyclic Silylene (NHSi)—Iron Complexes: Synthesis, Structures, and Catalytic Ability of an Isolable Hydridosilylene—Iron Complex. *J. Am. Chem. Soc.* **2013**, 135, 6703–6713.

(12) Cordero, B.; Gómez, V.; Platero-Prats, A. E.; Revés, M.; Echeverría, J.; Cremades, E.; Barragán, F.; Alvarez, S. Covalent Radii Revisited. *Dalton Trans.* **2008**, No. 21, 2832–2838.

(13) Li, H.; Aquino, A. J. A.; Cordes, D. B.; Hase, W. L.; Krempner, C. Electronic Nature of Zwitterionic Alkali Metal Methanides, Silanides and Germanides - A Combined Experimental and Computational Approach. *Chem. Sci.* **2017**, 8, 1316–1328.

(14) Lee, G.; West, R.; Muller, T. Bis[Bis(Trimethylsilyl)Amino]-Silylene, an Unstable Divalent Silicon Compound. *J. Am. Chem. Soc.* **2003**, 125, 8114–8115.

(15) Levason, W.; Reid, G.; Zhang, W. Coordination Complexes of Silicon and Germanium Halides with Neutral Ligands. *Coord. Chem. Rev.* **2011**, 255, 1319–1341.

(16) Al-Rafia, S. M. I.; McDonald, R.; Ferguson, M. J.; Rivard, E. Preparation of Stable Low-Oxidation-State Group 14 Element Amido-hydrides and Hydride-Mediated Ring-Expansion Chemistry of N-Heterocyclic Carbenes. *Chem. - Eur. J.* **2012**, 18, 13810–13820.

(17) Protchenko, A. V.; Birjumar, K. H.; Dange, D.; Schwarz, A. D.; Vidovic, D.; Jones, C.; Kaltsoyannis, N.; Mountford, P.; Aldridge, S. A Stable Two-Coordinate Acyclic Silylene. *J. Am. Chem. Soc.* **2012**, 134, 6500–6503.

(18) Lui, M. W.; Merten, C.; Ferguson, M. J.; McDonald, R.; Xu, Y.; Rivard, E. Contrasting Reactivities of Silicon and Germanium Complexes Supported by an N-Heterocyclic Guanidine Ligand. *Inorg. Chem.* **2015**, 54, 2040–2049.

(19) Driess, M.; Yao, S.; Brym, M.; van Wüllen, C.; Lentz, D. A New Type of N-Heterocyclic Silylene with Ambivalent Reactivity. *J. Am. Chem. Soc.* **2006**, 128, 9628–9629.

(20) Yao, S.; Xiong, Y.; Driess, M. Zwitterionic and Donor-Stabilized N-Heterocyclic Silylenes (NHSis) for Metal-Free Activation of Small Molecules. *Organometallics* **2011**, 30, 1748–1767.

(21) Meltzer, A.; Inoue, S.; Präsang, C.; Driess, M. Steering S–H and N–H Bond Activation by a Stable N-Heterocyclic Silylene: Different Addition of H₂S, NH₃ and Organoamines on a Silicon(II) Ligand versus Its Si(II)→Ni(CO)₃ Complex. *J. Am. Chem. Soc.* **2010**, 132, 3038–3046.

(22) Schmidt, M.; Blom, B.; Szilvási, T.; Schomäcker, R.; Driess, M. Improving the Catalytic Activity in the Rhodium-Mediated Hydroformylation of Styrene by a Bis(N-Heterocyclic Silylene) Ligand. *Eur. J. Inorg. Chem.* **2017**, 2017, 1284–1291.

(23) Witteman, L.; Evers, T.; Lutz, M.; Moret, M. A Free Silanide from Nucleophilic Substitution at Silicon(II). *Chem. - Eur. J.* **2018**, 24, 12236–12240.

(24) Filippou, A. C.; Steck, R.; Kociok-Köhn, G. Triazidogermeryl Complexes of Tungsten: Synthesis, Crystal Structure and Hydrolysis to a Metallocyclotrigermoxane. *J. Chem. Soc., Dalton Trans.* **1999**, No. 14, 2267–2268.

(25) (a) Contel, M.; Hellmann, K. W.; Gade, L. H.; Scowen, I. J.; McPartlin, M.; Laguna, M. Triamidogermeryl and Triamidostannaaurates(I): First Structural Characterization of a Ge–Au–Ge Unit. *Inorg. Chem.* **1996**, 35, 3713–3715. (b) Gade, L. H. Tripodal Triamidometallates of the Heavy Group 14 Elements: Inorganic Cages with Remarkable “Ligand Properties”. *Eur. J. Inorg. Chem.* **2002**, 2002, 1257–1268.

(26) Coste, S. C.; Vlasisavljevic, B.; Freedman, D. E. Magnetic Anisotropy from Main-Group Elements: Halides versus Group 14 Elements. *Inorg. Chem.* **2017**, 56, 8195–8202.

(27) Peerless, B.; Keane, T.; Meijer, A. J. H. M.; Portius, P. Homoleptic Low-Valent Polyazides of Group 14 Elements. *Chem. Commun.* **2015**, 51, 7435–7438.

(28) Steiner, A.; Stalke, D. Sodium Tri(Pyrazol-1-yl)-Germanate and -Stannate: New Tridentate ‘Claw-Ligands’ Containing Group 14 Metals. *J. Chem. Soc., Chem. Commun.* **1993**, No. 22, 1702–1704.

(29) Veith, M.; Schütt, O.; Huch, V. The First Crystal Structure of a Germanium(II) Amide with a Germanium–Lithium Bond and Its Behavior Towards Oxygen and Water. *Angew. Chem., Int. Ed.* **2000**, 39, 601–604.

(30) Fernández, I.; Oña-Burgos, P.; Armbruster, F.; Krummenacher, I.; Breher, F. ⁷Li,¹⁵N Heteronuclear Multiple Quantum Shift Correlation—a Fast and Reliable 2D NMR Method on Natural Abundant Nuclei. *Chem. Commun.* **2009**, 1, 2586–2588.

(31) Barnard, T. S.; Mason, M. R. Synthesis, Structure, and Coordination Chemistry of the Bicyclic π -Acid Phosphatri(3-Methyl-indolyl)Methane. *Organometallics* **2001**, 20, 206–214.

(32) (a) von Döbeneck, H.; Prietzel, H. Further Observations on Reaction between Aldehydes and Indole Derivatives. *Hoppe-Seyler's Z. Physiol. Chem.* **1955**, 299, 214–226. (b) Mason, M. R.; Barnard, T. S.; Segla, M. F.; Xie, B.; Kirschbaum, K. Di- and triindolymethanes: molecular structures and spectroscopic characterization of potentially bidentate and tridentate ligands. *J. Chem. Crystallogr.* **2003**, 33, 531–540.

(33) Steiner, A.; Stalke, D. Poly(Pyrazolyl)Germanium(II) and -Tin(II) Derivatives-Tuneable Monoanionic Ligands and Dinuclear Cationic Cages. *Inorg. Chem.* **1995**, 34, 4846–4853.

(34) Filippou, A. C.; Winter, J. G.; Kociok-Kohn, G.; Troll, C.; Hinz, I. Electron-Rich Trichlorogermeryl Complexes of Molybdenum and Tungsten Bearing a Cyclopentadienyl Ligand: Synthesis, Crystal Structures, and Cyclic Voltammetric Studies. *Organometallics* **1999**, 18, 2649–2659.

(35) Bent, H. A. An Appraisal of Valence-Bond Structures and Hybridization in Compounds of the First-Row Elements. *Chem. Rev.* **1961**, 61, 275–311.

(36) Khrustalev, V. N.; Antipin, M. Y.; Zemlyansky, N. N.; Borisova, I. V.; Ustynyuk, Y. A.; Lunin, V. V.; Izod, K. The Germanium(II) Ate Complex [Ph₃PiPr][Ge(OCOME)₃]: The First Structurally Characterized Compound Containing a Discrete [E^{14(II)}O₃][−] (E^{14(II)} = Si, Ge, Sn or Pb) Anion. *Appl. Organomet. Chem.* **2005**, 19, 360–362.

(37) Nogai, S.; Schriewer, A.; Schmidbaur, H. Reactions of Trichlorogermene HGeCl₃ and Dichlorogallane HGaCl₂ with Pyridine Donors. *Dalton Trans.* **2003**, 16, 3165–3171.

(38) Kersting, B.; Krebs, B. Syntheses and Structures of Germanium(II) and Germanium(IV) Thiolate and Selenolate Complexes: [Et₄N][Ge(SPh)₃], [Ph₄P][Ge(SePh)₃], [Ph₄P]₂[Ge₂(SCH₂-CH₂S)₃], Ge(S-4-MeC₆H₄)₄ and Ge(Se-2,4,6-Me₃C₆H₃)₄. Examples of the First Anionic Germanium(II) Complexes. *Inorg. Chem.* **1994**, 33, 3886–3892.

(39) Orlov, N. A.; Bochkarev, L. N.; Nikitinsky, A. V.; Zhiitsov, S. F.; Zakharov, L. N.; Fukin, G. K.; Khorshev, S. Ya. Synthesis and Crystal Structure of Cationic Complex of Ytterbium with Organogermanium Cuprate Anions {[Yb(THF)₆]²⁺[(Ph₃Ge)₂Cu]₂[−]}. 2THF. *J. Organomet. Chem.* **1997**, 547, 65–69.

(40) Zhao, N.; Zhang, J.; Yang, Y.; Zhu, H.; Li, Y.; Fu, G. β -Diketiminato Germylene-Supported Pentafluorophenylcopper(I) and -Silver(I) Complexes [LGe(Me)(CuC₆F₅)_n]₂ (n = 1,2), LGe[C-(SiMe₃)N₂]₂AgC₆F₅ and {LGe[C(SiMe₃)N₂](AgC₆F₅)₂}₂ (L = HC-[C(Me)N-2,6-iPr₂C₆H₃]₂): Synthesis and Structural Characterization. *Inorg. Chem.* **2012**, 51, 8710–8718.

(41) Ferro, L.; Hitchcock, P. B.; Coles, M. P.; Fulton, J. R. Reactivity of Divalent Germanium Alkoxide Complexes Is in Sharp Contrast to the Heavier Tin and Lead Analogues. *Inorg. Chem.* **2012**, 51, 1544–1551.

(42) Yadav, D.; Siwatch, R. K.; Sinhababu, S.; Nagendran, S. Aminotroponiminato(Chloro)Germylene Stabilized Copper(I) Iodide Complexes: Synthesis and Structure. *Inorg. Chem.* **2014**, 53, 600–606.

(43) Yadav, D.; Kumar Siwatch, R.; Sinhababu, S.; Karwasara, S.; Singh, D.; Rajaraman, G.; Nagendran, S. Digermylene Oxide Stabilized Group 11 Metal Iodide Complexes. *Inorg. Chem.* **2015**, *54*, 11067–11076.

(44) York, J. T.; Young, V. G.; Tolman, W. B. Heterobimetallic Activation of Dioxygen: Characterization and Reactivity of Novel Cu(I)–Ge(II) Complexes. *Inorg. Chem.* **2006**, *45*, 4191–4198.

(45) Hlina, J.; Arp, H.; Walewska, M.; Flörke, U.; Zangger, K.; Marschner, C.; Baumgartner, J. Coordination Chemistry of Cyclic Disilylated Germylenes and Stannylenes with Group 11 Metals. *Organometallics* **2014**, *33*, 7069–7077.

(46) Orlov, N. A.; Bochkarev, L. N.; Nikitsky, A. V.; Kropotova, V. Y.N.; Zakharov, L. N.; Fukin, G. K.; Khorshev, S. Y. Synthesis of Germylecopper Compounds by Hydride Method. Crystal Structure of $(C_6F_5)_3GeCu(PPh_3)_2$. *J. Organomet. Chem.* **1998**, *560*, 21–25.

(47) Piers, E.; Lemieux, R. E. D. Reaction of (Trimethylgermyl) Copper(I) Dimethyl Sulfide with Acyl Chlorides: Efficient Syntheses of Functionalized Acyltrimethylgermanes. *Organometallics* **1995**, *14*, 5011–5012.

(48) Glockling, F.; Hooton, K. A. Triphenylgermyl Complexes of Copper, Silver, and Gold. *J. Chem. Soc.* **1962**, 2658–2661.

(49) Barnard, T. S.; Mason, M. R. Hindered Axial–Equatorial Carbonyl Exchange in an $Fe(CO)_4(PR_3)$ Complex of a Rigid Bicyclic Phosphine. *Inorg. Chem.* **2001**, *40*, 5001–5009.

(50) Couzijn, E. P. A.; Slootweg, J. C.; Ehlers, A. W.; Lammertsma, K. Stereomutation of Pentavalent Compounds: Validating the Berry Pseudorotation, Redressing Ugi's Turnstile Rotation, and Revealing the Two- and Three-Arm Turnstiles. *J. Am. Chem. Soc.* **2010**, *132*, 18127–18140.

(51) Armarego, W. L. F.; Chai, C. L. L. *Purification of Laboratory Chemicals*, 5th ed.; Butterworth-Heinemann: Amsterdam, 2003.

(52) Fulmer, G. R.; Miller, A. J. M.; Sherden, N. H.; Gottlieb, H. E.; Nudelman, A.; Stoltz, B. M.; Bercaw, J. E.; Goldberg, K. I. NMR Chemical Shifts of Trace Impurities: Common Laboratory Solvents, Organics, and Gases in Deuterated Solvents Relevant to the Organometallic Chemist. *Organometallics* **2010**, *29*, 2176–2179.

(53) Frisch, M. J.; Trucks, G. W.; Schlegel, H. B.; Scuseria, G. E.; Robb, M. A.; Cheeseman, J. R.; Scalmani, G.; Barone, V.; Mennucci, B.; Petersson, G. A.; Nakatsuji, H.; Caricato, M.; Li, X.; Hratchian, H. P.; Izmaylov, A. F.; Bloino, J.; Zheng, G.; Sonnenberg, J. L.; Hada, M.; Ehara, M.; Toyota, K.; Fukuda, R.; Hasegawa, J.; Ishida, M.; Nakajima, T.; Honda, Y.; Kitao, O.; Nakai, H.; Vreven, T.; Montgomery, J. A., Jr.; Peralta, J. E.; Ogliaro, F.; Bearpark, M.; Heyd, J. J.; Brothers, E.; Kudin, K. N.; Staroverov, V. N.; Keith, T.; Kobayashi, R.; Normand, J.; Raghavachari, K.; Rendell, A.; Burant, J. C.; Iyengar, S. S.; Tomasi, J.; Cossi, M.; Rega, N.; Millam, J. M.; Klene, M.; Knox, J. E.; Cross, J. B.; Bakken, V.; Adamo, C.; Jaramillo, J.; Gomperts, R.; Stratmann, R. E.; Yazyev, O.; Austin, A. J.; Cammi, R.; Pomelli, C.; Ochterski, J. W.; Martin, R. L.; Morokuma, K.; Zakrzewski, V. G.; Voth, G. A.; Salvador, P.; Dannenberg, J. J.; Dapprich, S.; Daniels, A. D.; Farkas, O.; Foresman, J. B.; Ortiz, J. V.; Cioslowski, J.; Fox, D. J. *Gaussian 09*, Revision D.01; Gaussian, Inc.: Wallingford, CT, 2013.